Materials and Structures/Matériaux et Constructions, Vol. **34**, April 2001, pp 155-162

Experimental study of the behaviour of reinforced high-strength concrete short corbels

M. Bourget[1], Y. Delmas[1] and F. Toutlemonde[2]

(1) Groupe Mécanique, Matériaux, Structures, Université de Reims Champagne-Ardenne, rue des Crayères, BP 1037, 51687 Reims Cedex 2, France

(2) Structures Department, Laboratoire Central des Ponts et Chaussées, 58 bd Lefebvre, Paris Cedex 15, France

Paper received: June 6, 2000; Paper accepted: October 10, 2000

ABSTRACT

Within the framework of the French National Project BHP 2000 (the BHP 2000 project is detailed in Toutlemonde *et al.* [1]), seven high-strength reinforced concrete short corbels were tested using concrete from 70 MPa to 120 MPa. The behaviour of a test specimen is characterised by the crack pattern and by LVDT and gauges measurements. The results show the influence of the concrete strength and that of the reinforcement quantity (Bourget and Delmas [2]). The failure conventional shear stresses computations with the relations proposed by B. Fouré [3] show that these relations are adapted to the strength evaluation of the short corbels with a safety coefficient.

RÉSUMÉ

Dans le cadre du Projet National français BHP 2000 (le projet BHP 2000 est détaillé dans Toutlemonde et al. *[1]), sept consoles courtes en béton armé réalisées en bétons hautes performances de 70 à 120 MPa ont été testées. Le comportement d'un corps d'épreuve est caractérisé par le relevé de fissuration et par des mesures effectuées avec des jauges de déformation et un capteur LVDT. Les résultats montrent l'influence de la résistance du béton et du ferraillage (Bourget et Delmas [2]). Les valeurs à la rupture de la contrainte conventionnelle de cisaillement calculée en utilisant les relations proposées par B. Fouré [3] montrent que ces relations sont adaptées à l'évaluation de la résistance des consoles avec un coefficient de sécurité.*

1. INTRODUCTION

Until recently, the compressive strength of concrete was limited to 30 MPa by the French design code concerning short reinforced concrete corbels (appendix E 6 of the BAEL 91 provision [4]). Work made by the AFREM group on concrete whose compressive strength varies from 40 to 80 MPa [5] shows that the high-strength concrete and the normal concrete behave differently. This is mainly due to the progressively decreasing role of aggregate interlock when f_c increases. Thus, the expression of the failure stress of the short corbels has to be modified for the design of high-strength concrete corbels.

Fouré [3] proposes relations for the high-strength concrete corbel design. These relations ensure the continuity with those of the BAEL 91 code. An experimental program of seven test specimens has been organised for the evaluation of these relations.

The experimental corbel failure modes can be either crushing of the concrete in the compressive strut of the corbel (concrete crushing mode) or yielding of the main reinforcement (tension mode) or brutal split of the corbel in two pieces (diagonal splitting mode) or shearing at the interface between the corbel and the column (shearing mode). The behaviour of a corbel is generally associated to a strut and tie structure and the theoretical failure modes are only concrete crushing or yielding of the main reinforcement. Experimentally, the shearing mode has rarely been observed and generally the brutal split of the corbel in two pieces occurs after the main reinforcement has yielded.

2. CHARACTERISTICS OF THE SPECIMENS

The aim of the experimental program is to study the influence of concrete strength. Three different concrete compositions established by F. De Larrard (De Larrard *et al.* [6]) were used with a mean strength of 80, 100, and 120 MPa respectively.

The test specimens were gathered in 2 series. The first one consisted of high-level reinforcement corbels:

Editorial Note
The LCPC is a RILEM Titular Member.

Table 1 - Details of the reinforcements of the test specimens

Corbel	Main reinforcement			
	Number of bars	Diameters mm	ρ_s %	f_{es} MPa
C1-80	2	8	0.21	550
C2-80	2	12	0.49	550
C3-80	2	16	0.90	525
C1-100	2+2	12-12	1.04	550
C2-100	2	12	0.49	550
C1-120	2	14	1.24	550
C2-120	2	14	1.24	550
Corbel	Secondary reinforcement			
	Number of bars	Diameters mm	ρ_s %	f_{es} MPa
C1-80	2	6	0,12	500
C2-80	2	8	0,22	550
C3-80	2+2+2	8-8-8*	0,68	550
C1-100	2+2+2	10-10-8*	0,95	550
C2-100	2	8	0,22	550
C1-120	2+2+2	12-12-10*	1,28	550
C2-120	2+2+2	12-12-10*	1,28	550

* *Stirrups at a spacing of 6.5 cm center to center.*

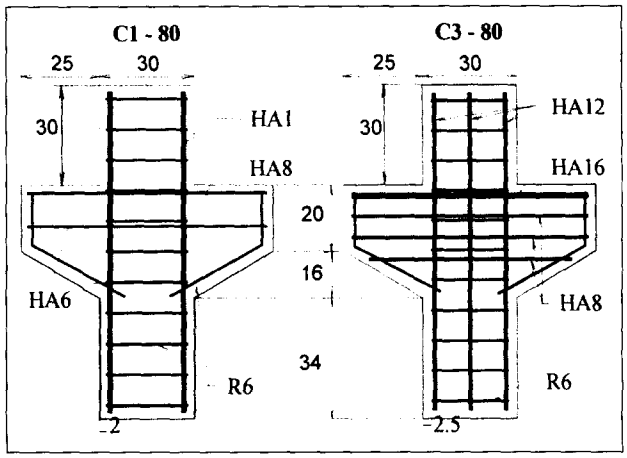

Fig. 1 - Details of two test specimens. The dimensions are in centimeters. HA12 is a deformed bar of 12 mm, R6 is a round bar of 6 mm diameter.

Table 2 - Characteristics of the concrete

Corbel	f_c MPa	δ	R_t MPa	E GPa	ν
C1-80	70	0.37	-	-	-
C2-80	70	0.37	-	-	-
C3-80	91	0.25	3.6	47.8	0.22
C1-100	106	0.25	3.6	47.9	0.25
C2-100	110	0.37	4.0	47.9	0.25
C1-120	132	0.25	3.8	58.1	0.25
C2-120	132	0.39	4.0	55.9	0.26

C3-80, C1-100, C1-120 and C2-120. For this series, the diameters of the reinforcement bars were computed with the relations proposed by Fouré in order to obtain corbels sufficiently reinforced so that the failure could occur by concrete crushing. The second series consisted of specimens with lower-level reinforcement quantity: C1-80, C2-80, C2-100.

The reinforcement of the test specimens is detailed in Table 1 and two examples are presented in Fig. 1. An anchor bar was welded to primary and secondary steel. The diameter of the frame bars was 6 mm.

One test specimen and six 320 mm x 160 mm diameter cylinders were prepared from each batch of concrete. The test specimen and the concrete cylinders were left seven days with a plastic film protection. Then, they were demoulded and left without any curing procedure in the laboratory. Young's modulus and Poisson's ratio were measured on a cylinder of each batch of concrete (except for test specimens C1-80 and C2-80). The characteristics of the concrete are presented in Table 2.

3. TESTING PROCEDURE

3.1 Test specimen instrumentation

Two corbels of each test specimen were instrumented. For the tensile stress evaluation, a gauge was bonded on the main reinforcement at the corbel-column interface. The other gauges were placed on the concrete surface, near the corbel-column interface, in order to evaluate the stress tensors: three gauges were located near the corbel sloping face and three others were located at middle height. In addition, a displacement transducer LVDT was used to measure the horizontal extension of the test specimen. The LVDT measures the extension between two points beyond the bearing plate (See Fig. 2). The horizontal extension depends on the width of the cracks and on the deflection of the test specimen.

3.2 Test arrangement

The specimens were tested in an inverted position as shown in Fig. 2.

The load was applied at the top of the column. A bearing plate of 50 mm is inserted, between the corbel and the roller support, to distribute the load on the corbel support area. To limit the effect of the concrete surface roughness, a 5-mm-thick plate of plywood was laid out between the corbel and the bearing plate. The distance between the medium of the bearing plate and the corbel-column interface is 82 mm ($\delta \approx 0.25$) or 125 mm ($\delta \approx 0.37$).

3.3 Loading procedure

The loading system was monitored according to the jack displacement. The speed was of 0.4 mm/minute until the first crack appeared, then, the speed was of 0.2

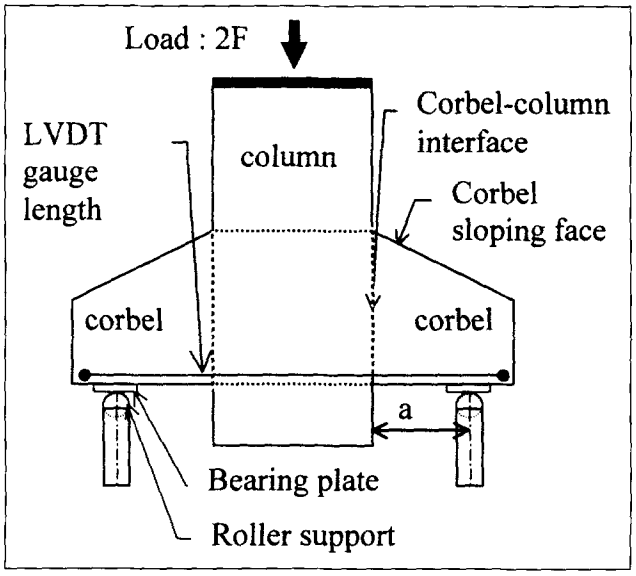

Fig. 2 – Test arrangement.

mm/minute to allow a progressive propagation of the cracks. As the load increased slowly during the test, the crack pattern was recorded continuously during the test (without stop of loading). The measured values were recorded every second.

4. EXPERIMENTAL RESULTS

4.1 Crack patterns

The crack patterns, presented in Fig. 3, indicated three crack locations during the loading:
– Cracks near the corbel-column interface.
– Cracks from the support areas to the corbel-column interface.
– Cracks near the intersection of the column and the corbel sloping face.

Cracks near the corbel-column interface never caused the corbel failure.

For the less reinforced test specimens C1-80, C2-80 and C2-100, the failure resulted from crack propagation from the support areas to the corbel-column interface. The crack reached the interface at the intersection of the column and the corbel sloping face. These failures corresponded to the diagonal splitting failure mode.

In all other cases, the failure was partly due to cracks located between the support areas and the corbel-column interface. These cracks crossed the interface before the intersection of the corbel sloping face. After their propagation, the corbel failure results from the failure of the remained uncracked concrete area near the intersection of the column and the corbel sloping face. This failure mode was associated with the concrete crushing in the compressive strut.

Thus, the corbel failure seems to occur according to the following scenario:

First, the cracks propagate near the corbel-column interface without causing the corbel failure. Then, the cracks propagate between the bearing plate and the corbel-column interface with an average orientation of 71° ± 5° with respect to the horizontal. Either these cracks cut the corbel-column interface at the intersection with the corbel sloping face or they cut the interface before. In the first case, the corbel is maintained with the column only by its reinforcements and the failure occurs according to these cracks (diagonal splitting mode). In the second case, the corbel failure occurs after the failure of the remained uncracked concrete near the sloping face of the corbel (concrete crushing mode).

4.2 Strain measurements on main reinforcement

Two gauges were placed symmetrically on both sides of the column on the main reinforcement (one of the two gauges did not function during the test on specimen C3-80). The gauges were located 10 mm inside the column. The strain versus the conventional shear stress is presented in Fig. 4.

The main reinforcement strain evolution has been described as four phases (see Fig. 5):
1. The main reinforcement strain varies linearly according to the conventional shear stress: there is no cracking.
2. The strain variation is no longer a linear function of the conventional shear stress: the development of the cracks starts at the corbel-column interface.
3. The strain variation is again linear but with discontinuities: the cracks develop from the support areas. The discontinuities seem to be related to the cracking development.
4. There is no linear dependence: the stress in main reinforcement has reached the yield strength of the steel.

These 4 phases correspond to those reported by Khadraoui [7], Kriz and Raths [8], Foster *et al.* [9, 10] and Robinson [11].

The fourth phase is not present if the corbel failure occurs before the stress in the main reinforcement has reached the yield stress.

Fig. 4 shows that for test specimens C1-80 and C2-80, the main reinforcement yielding is very quickly reached. The evolutions of the main reinforcement strain versus the conventional shear stress show that the failure of test specimens C1-80, C2-80, C3-80 and C2-100 occurred after the main reinforcement had yielded. It is also the case for test specimen C1-100 because the failure occurred on the side of the gauge j1. The failure of test specimens C1-120 and C2-120 occurred before the main reinforcement had yielded (phase 4 is not present).

The comparison of the evolutions of the main reinforcement strain shows that the reinforcement quantity of the test specimens is more determinant than δ and the concrete strength.

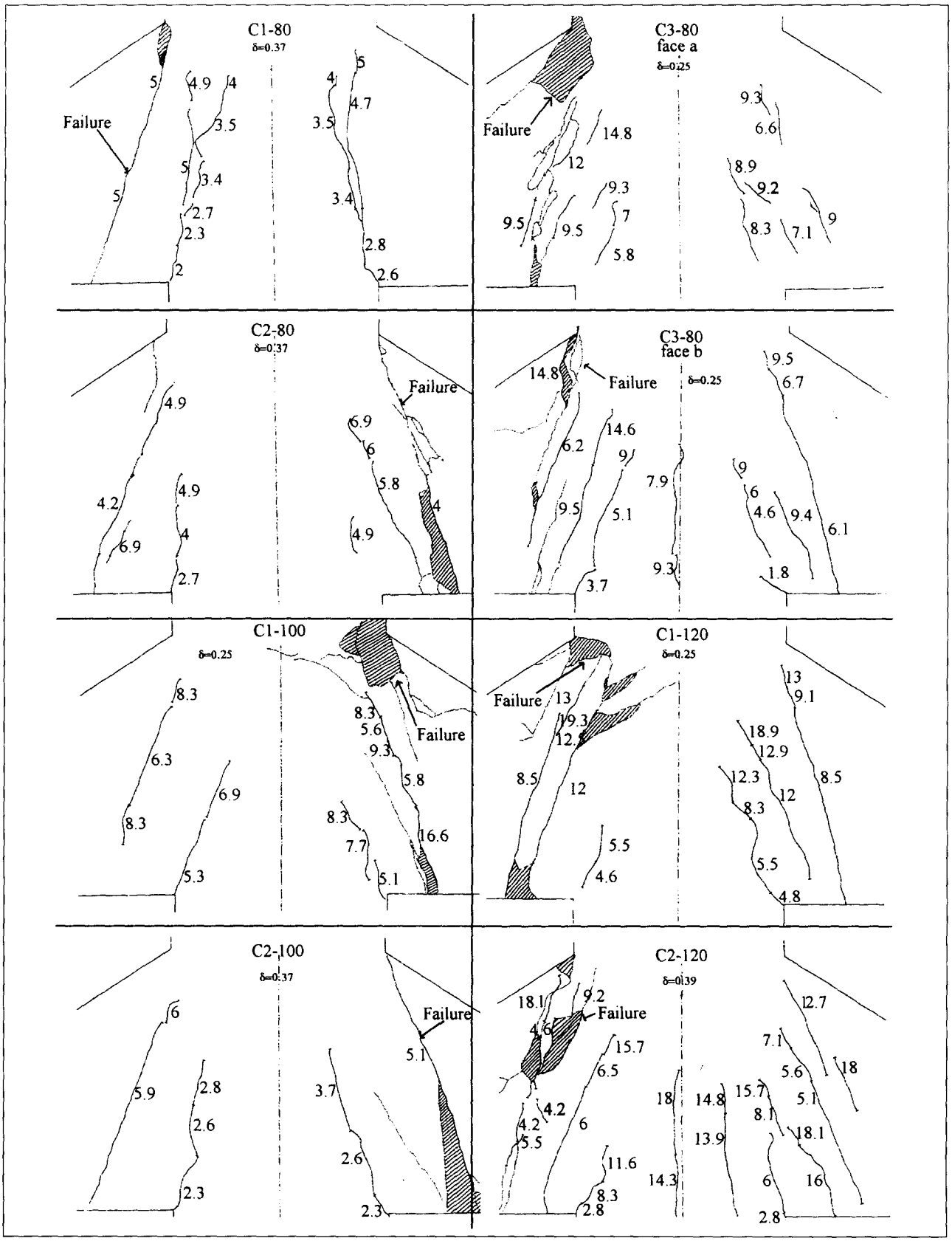

Fig. 3 – Crack patterns. The conventional shear stress value corresponding to the crack onset is indicated in MPa. The full features correspond to cracking during the test. The lighter features and the hatchings characterize the concrete chipping and the cracks which appeared during the test specimen failure. Excepted for test specimen C3-80, only one face is presented.

4.3 Strain measurements on concrete

Young's modulus and Poisson's ratio of concrete, presented in Table 2, are used to compute the components σ_{ij} of the stress tensor at middle height of column-corbel interface and near the intersection of the column and the corbel sloping face. These tensors are then diagonalized in order to obtain the principal stresses σ_1 and σ_2.

The strain gauge values are interpreted in terms of states of stress. The measured state of stress corresponds

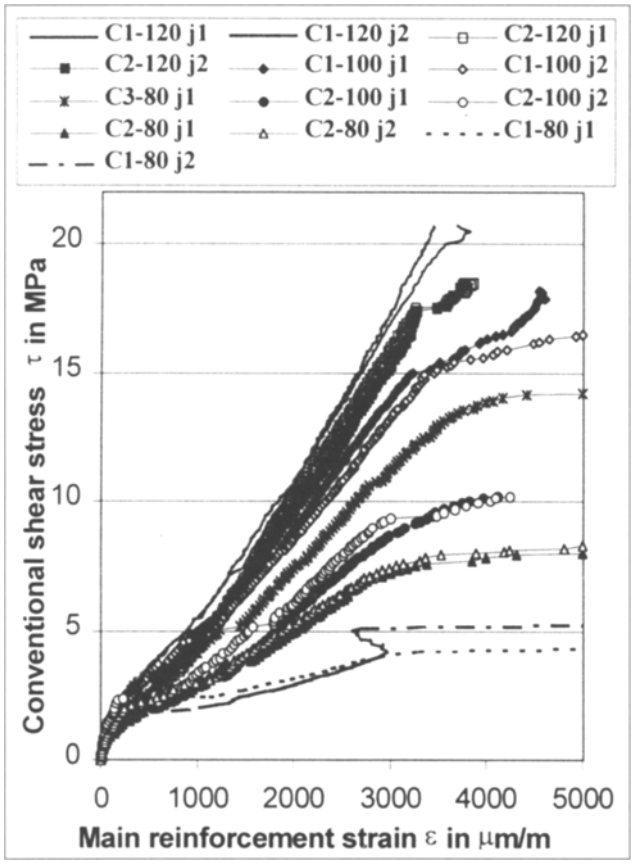

Fig. 4 – Evolutions of the conventional shear stress versus the main reinforcement strain.

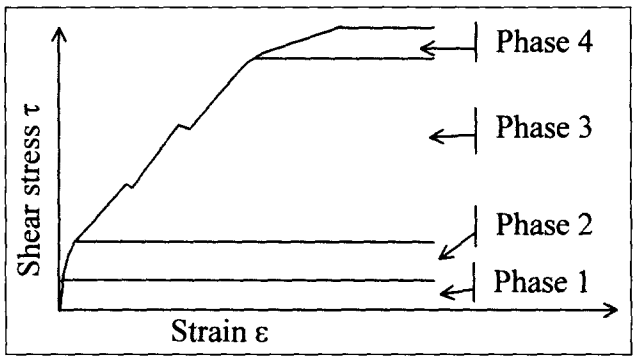

Fig. 5 – Diagram of the strain versus conventional stress evolution in 4 phases.

to a principal stress σ_1 in compression. The second principal stress σ_2 can be either in compression or in tension.

Nevertheless, it is necessary to keep in mind that the strain values measured by the gauges relate to uncracked or cracked concrete. Thus, σ_2 higher than 5 MPa means that the concrete is cracked.

The gauges located at middle height of the corbel-column interface indicate generally a state of stress σ_2 in tension until cracking. Nevertheless, σ_2 for one of the two corbels, at middle height can be in compression (C2-80, C3-80, C2-120 and C1-100).

The gauges located on test specimen C3-80 (see Figs. 6 and 7) were the less disturbed by the cracking. The strain values corresponded to σ_2 in compression until the failure. During the test specimen failure, σ_1 = -64 MPa with σ_2 growing quickly until it reached 5 MPa.

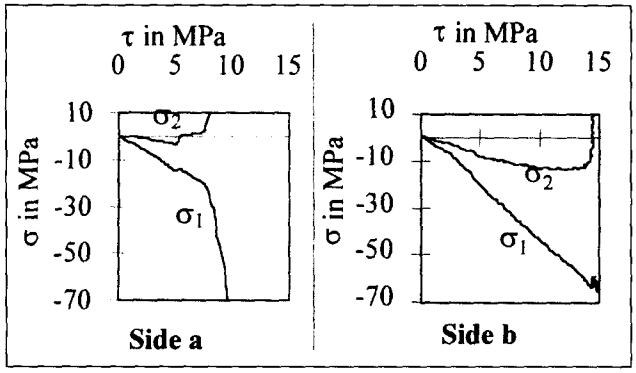

Fig. 6 – Test specimen C3-80 - Evolution versus conventional shear stress of the principal stresses near the intersection of the column and the corbel sloping face.

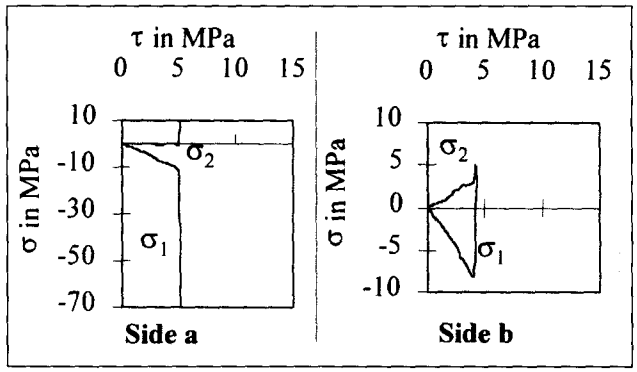

Fig. 7 – Test specimen C3-80 - Evolution versus conventional shear stress of the principal stresses at the middle-height of the corbel-column interface.

The increase in σ_2 in side b of Fig. 6 corresponds to the increase in the main reinforcement strain at the yield point. Thus, for test specimen C3-80, the main reinforcement has yielded just before the concrete crushing in the compressive strut.

It is difficult to determine with this method if the test specimen failed by concrete crushing before or after the main reinforcement has yielded because generally the gauges were cut by a crack at low conventional shear stress value (3 to 5 MPa).

4.4 LVDT measurements

The LVDT was not used for test specimens C1-80 and C2-80. For the other specimens, the extension of the horizontal distance versus the conventional shear stress is presented in Fig. 8.

As for the evolution of the main reinforcement strain, the least reinforced specimen (C2-100) is characterised by the most important extension of the horizontal distance. The most reinforced specimen, tested with $\delta = 0.25$, presents the lowest extension.

4.5 Tests results

The identification of the experimental failure mode is not obvious. For example, test specimen C2-100 failed

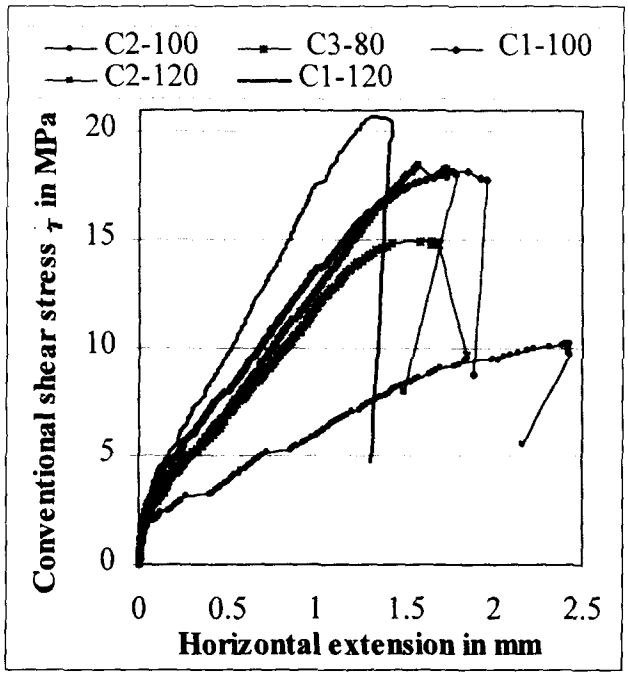

Fig. 8 – Evolutions of the conventional shear stress versus the horizontal extension.

by yielding of the main reinforcement (as shown in Fig. 4) and the crack pattern (presented in Fig. 3) indicates diagonal splitting failure mode. Foster proposed a clear definition of the experimental failure mode: the primary failure mode is in tension which corresponds to corbel failure after the main reinforcement has yielded. The other modes, diagonal splitting and concrete crushing (identified with the crack pattern), are considered only if the main reinforcement has not yielded.

For each test specimen, the experimental failure mode proposed in Table 3 is first defined with the evolution of the main reinforcement strain versus conventional shear stress. The crack pattern is then considered if the main reinforcement has not yielded or as an indication of the concrete strut failure mode.

5. HIGH-STRENGTH CONCRETE CORBEL STRENGTH PROPOSED BY FOURÉ [3]

The ultimate conventional shear stress τ_{uth} evaluated with the BAEL 91 relations presents three limits: $\tau_{uth} \leq 4$ MPa, $f_c \leq 30$ MPa and $\delta \geq 0.25$. The full advantage of high-strength concrete is not available by the designer with the first and the second limits. Thus, Fouré proposes modifications while ensuring continuity with the relations of the BAEL 91 for the concrete of 40 MPa:

δ is limited to 0.25 and the concrete strength is higher than 40 MPa.

$\tau_{u,th}$, is the minimum of τ_u^b and τ_u^f.

τ_u^f, the failure stress by yielding of the main reinforcement, is expressed by:

$$1 \geq \delta > 0.6 : \tau_u^f = \frac{0.7}{\delta}\rho_s \frac{f_{es}}{\gamma_s}\left(1+\frac{0.1}{\delta}\right)$$

$$0.6 \geq \delta > 0.25 : \tau_u^f = \frac{2.4}{\delta}\rho_s \frac{f_{es}}{\gamma_s}\left(0.1+0.4\delta\right)$$

with $\gamma_s = 1.15$ for the design and $\gamma_s = 1$ for the comparison with experimental results.

The expression of τ_u^b, the failure stress by concrete crushing, is expressed by:

$$1 \geq \delta \geq 0.41 : \tau_u^b = \tau_u^{b1} = 0.077\left(2+\frac{1}{\delta}\right)f_c^{2/3}$$

$$0.41 \geq \delta \geq 0.25 : \tau_u^b = \tau_u^{b2} = \tau_u^{b1} - 0.9\left(\frac{1}{\delta}-2.44\right)$$

The quantity of secondary reinforcement is evaluated with:

$$\frac{\rho_r f_{er}}{\rho_s f_{es}} = \frac{1}{4}\left(\frac{1.9\tau_{uth}}{f_c^{\frac{1}{2}}}+\frac{1}{\delta}-1\right)$$

The failure stresses computations for the test specimens are presented in Table 3.

The theoretical tension failure mode occurs for the less reinforced test specimens which have experimentally failed after the main reinforcement has yielded. For these specimens, the values of τ_{uexp}/τ_{uth} (see Table 3) are the most variable (from 2 to 3). The most reinforced specimens are associated with the theoretical failure mode of concrete crushing and with low variations of τ_{uexp}/τ_{uth} (from 2.1 to 2.3).

The results show that the relations proposed by Fouré estimate the corbel failure stress with a safety coefficient. By analogy with the safety coefficient γ_s on steel, a safety coefficient γ_b on the concrete behaviour can be introduced. An additional safety can be considered on the corbel strength evaluation due to the simplification of the model and the uncertainties related to the characteristics (geometry and load value) of the tests.

Table 3 – Theoretical and experimental characteristics of the corbel failure (T = Tension, D = Diagonal splitting, C = Concrete crushing)

Corbel	τ_u^b MPa	τ_u^f MPa	τ_{uth} MPa	Theoretical failure mode	F_{uexp} kN	τ_{uexp} MPa	$\frac{\tau_{uexp}}{\tau_{uth}}$	Experimental failure mode
C1-80	5.89	1.89	1.89	T	282	5.61	2.97	TD
C2-80	5.88	4.29	4.29	T	448	8.94	2.09	TD
C3-80	7.91	9.08	7.91	C	807	16.45	2.08	TC
C1-100	8.86	10.91	8.86	C	980	20.23	2.28	TC
C2-100	8.02	4.29	4.29	T	550	10.98	2.56	TD
C1-120	10.45	12.94	10.45	C	1117	23.12	2.21	C
C2-120	8.98	10.73	8.98	C	997	20.64	2.30	C

Table 4 – Characteristics, ultimate conventional stresses and failure modes of tests specimens from Foster [10] and this study

						Foster		Fouré		
Corbel	f_c MPa	δ	ρ_s %	f_{es} MPa	τ_{uexp} MPa	τ_{uexp} τ_{uth}	Th. Fail. mode	τ_{uexp} τ_{uth}	Th. Fail. mode	Exp. Fail. mode
C1-80	70	0.37	0.21	550	5.61	2.20	T	2.97	T	T
C2-80	70	0.37	0.49	550	8.94	1.55	T	2.09	T	T
C3-80	91	0.25	0.90	525	16.45	1.39	C	2.08	C	T
C1-100	106	0.25	1.04	550	20.23	1.45	C	2.28	C	T
C2-100	110	0.37	0.49	550	10.98	1.91	T	2.56	T	T
C1-120	132	0.25	1.24	550	23.12	1.39	C	2.21	C	C
C2-120	132	0.39	1.24	550	20.64	1.47	T	2.30	C	C
PB2	105	0.30	4.93	495	15.33	1.09	C	2.45	C	C
PC2	53	0.30	0.90	420	13.87	1.54	C	2.79	C	C
PD2	71	0.40	2.46	450	12.80	1.06	C	2.18	C	C
PE2	71	1.00	4.52	480	10.52	1.17	C	2.66	C	C
PF2	105	0.30	0.90	420	14.00	1.54	T	2.09	T	T
PG1	45	0.60	2.51	415	8.99	1.26	C	2.52	C	C
PG2	94	0.60	2.51	415	14.00	1.07	C	2.41	C	C
SC1-3	90	0.50	0.90	430	9.33	1.55	T	1.67	T	T
SC2-1	62	0.55	2.51	430	13.07	1.25	C	2.72	C	C
SD1	95	0.50	2.51	430	13.33	1.13	C	2.09	C	C
SD2	65	0.50	2.51	430	13.33	1.22	C	2.69	C	C
					Mean M:	1.40		2.37		
					Standard deviation S:	0.30		0.33		
					S/M:	0.21		0.14		

6. VALIDATION WITH FOSTER'S STUDY

The most important contribution on high-strength corbel behaviour has been presented by Foster [9, 10]: 30 corbels had been tested and the ultimate loads had been predicted with a plastic struss model which provided a good tool for designing corbels. Therefore, it seemed interesting to validate the model proposed by Fouré with Foster's results. Foster's test specimens without secondary reinforcement were not considered because all design codes specify a minimum quantity of horizontal stirrups. Moreover, the theoretical failure modes are tension or concrete crushing, thus only the corbels experimentally failed by these failure modes were considered.

The plastic struss model proposed by Foster can be reminded with three equations:

$\tau^{f}_{uFos} = \rho_s f_{es} l_w/(d - (d^2 - l_w a - l_w^2)^{1/2})$.

$\tau^{c}_{uFos} = \min((l_w/d)(1.25 - (f_c/500) - 0.72\delta + 0.18\delta^2), 0.85)$.

$\tau_{u\,thFos} = \min(\tau^{f}_{u}, \tau^{c}_{u})$.

where τ^{f}_{uFos} and τ^{c}_{uFos} are the conventional failure stress by respectively yielding of the main reinforcement and crushing of the concrete strut; $\tau_{u\,thFos}$ is the ultimate conventional stress.

The results presented in Table 4 show that M, the mean value of τ_{uexp}/τ_{uth}, is closer to 1 with Foster's model and the lowest value of S/M, the variation coefficient, is obtained with Fouré's model. Thus, these results validate Fouré's model and confirm that this model with safety coefficients will be pertinent.

7. CONCLUSIONS

The tests on the high-strength (concrete from 70 to 130 MPa) short corbels and the comparison with Foster's study validate the high-strength concrete corbel failure stresses relations proposed by Fouré [3]: the ultimate conventional shear stress is reasonably evaluated with a safety factor which is more variable for the less reinforced specimens than for the most reinforced specimens. The safety factor must be studied to be explicitly introduced in the relations.

The experimental corbel failure mode is first defined with the evolution of the main reinforcement strain versus conventional stress: if the main reinforcement has yielded the failure mode is tension failure; if it is not the case the crack pattern indicates the failure mode by concrete crushing or by diagonal splitting.

The crack patterns show that the failure of the concrete strut is due to the propagation of the cracks from the support zones to the corbel-column interface. If the intersection of these cracks and the corbel-column interface is closed to the corbel sloping face, the concrete strut fails in diagonal splitting mode. In the other cases, the strut failure occurs after the failure of the remained healthy concrete zone close to the corbel sloping face.

REFERENCES

[1] Toutlemonde, F., Brazillier, D. and de Larrard, F., 'Recent advances in France in High Performance Concrete technology' Proceedings of SEWC'98, San Francisco, July 98, "T185-3", (Structural Engineering World Wide, Elsevier Sciences, 1998).

[2] Fouré, B., 'Justifications sous sollicitations tangentes', *Bulletin des Laboratoires des Ponts et Chaussées* **spécial XIX** (1996) 43-52.

[3] Bourget, M. et Delmas, Y., 'Dimensionnement des consoles courtes en BTHP', Rapport d'étude du PN BHP 2000 (1998).

[4] BAEL 91 annexe E.6 Consoles courtes.

[5] 'Extension du domaine d'application des règlements de calcul BAEL/BPEL aux bétons à 80 MPa', *Bulletin des Laboratoires des Ponts et Chaussées* **spécial XIX** (1996).

[6] de Larrard, F. et Baroghel-Bouny, V., 'Vieillissement des bétons en milieu naturel : une expérimentation pour le XXI^{e} siècle. I : Généralités et caractéristiques mécaniques des bétons', *Bulletin des Laboratoires des Ponts et Chaussées* **225** (2000).

[7] Khadraoui, A., 'Analyse et comportement mécanique des consoles courtes en béton armé', Thèse de l'Université de Reims Champagne-Ardenne, (1998).

[8] Kriz, L. B. and Raths, C. H., 'Connections in precast concrete structures: Structures-strength of corbels', *PCI Journal* **10** (1965) 16-60.

[9] Foster, S. and Gilbert, R., 'The design of nonflexural members with normal and high-strength concretes', *ACI Structural Journal* (January-February 1996) 3-10.

[10] Foster, S., Powel, R. and Selim, H., 'Performance of high-strength concrete corbels', *ACI Structural Journal* (September-October 1996) 555-563.

[11] Robinson, J. R., 'Éléments constructifs spéciaux du béton armé' (Éditions EYROLLES. 1975).

NOTATION

d: effective depth: vertical distance from the main reinforcement center to the intersection of the column and the sloping face of the corbel.
a: shear span: distance between vertical load and corbel-column interface.
$\delta = a/d$.
b: test specimen thickness (15 cm).
l_w: effective width of the bearing plate.
2F: vertical load applied on the column of test specimen.
F_{uexp}: ultimate load of the short corbel.
$\tau = F/bd$: conventional shear stress.
$\tau_{u\,th}$: ultimate theoretical conventional shear stress.
$\tau_{u\,exp}$: ultimate experimental conventional shear stress.
ρ_s: A_s/bd where A_s is the main reinforcement area.
ρ_r: A_r/bd where A_r is the secondary reinforcement area.
γ_s: safety coefficient on steel yielding.
f_{es}: yield stress of the main reinforcement.
f_{er}: yield stress of the secondary reinforcement.
f_c: compressive strength of concrete.
Rt: tensile splitting strength of concrete.
E: Young's modulus of concrete.
ν: Poisson's ratio of concrete.

ACKNOWLEDGEMENTS

The tests reported herein were carried out at the IUT (University Institute of Technology) of Béthune. The National Project BHP 2000 is gratefully acknowledged for its financial support. We thank Mr. Fouré and Pr. Buyle-Bodin for their support and advice.